

CHEMISTRY

A European Journal

A Journal of



Accepted Article

Title: Ultrafast charge separation in triphenylamine-BODIPY derived triads carrying centrally positioned, highly electron deficient, dicyanoquinodimethane or tetracyanobutadiene acceptors

Authors: Francis D'Souza, Prabhat Gautam, Rajneesh Misra, and Michael Thomas

This manuscript has been accepted after peer review and appears as an Accepted Article online prior to editing, proofing, and formal publication of the final Version of Record (VoR). This work is currently citable by using the Digital Object Identifier (DOI) given below. The VoR will be published online in Early View as soon as possible and may be different to this Accepted Article as a result of editing. Readers should obtain the VoR from the journal website shown below when it is published to ensure accuracy of information. The authors are responsible for the content of this Accepted Article.

To be cited as: *Chem. Eur. J.* 10.1002/chem.201701604

Link to VoR: <http://dx.doi.org/10.1002/chem.201701604>

Supported by
ACES

WILEY-VCH

Ultrafast charge separation in triphenylamine-BODIPY derived triads carrying centrally positioned, highly electron deficient, dicyanoquinodimethane or tetracyanobutadiene electron acceptors

Prabhat Gautam,^[a] Rajneesh Misra,*^[a] Michael B. Thomas,^[b] Francis D'Souza*^[b]

Abstract: A series of triphenylamine (TPA) substituted BODIPYs **1–3** have been newly designed and synthesized by the Pd-catalysed Sonogashira cross-coupling and [2+2] cycloaddition–retroelectrocyclization reaction in good yields. This procedure yielded highly electron deficient tetracyanobutadiene (TCBD) or dicyanoquinodimethane (DCNQ) electron acceptor units centrally located at the TPA-BODIPY system. As a consequence, significant perturbation of the photonic and electronic properties was observed. The triads **2** and **3** showed red-shifted absorption in addition to a strong

charge transfer type absorption in the case of **3**. The electrochemical studies revealed multi-redox processes involving the TPA, TCBD or DCNQ and BODIPY entities. The computational studies were performed at the B3LYP/6-31G** level to elucidate the geometry and electronic structures. An energy level diagram established for triads **2** and **3** revealed that the photoinduced charge separation from the ¹BODIPY* is thermodynamically possible. In addition, charge transfer from TPA to TCBD in **2** and DCNQ in **3** were also possible. These charge transfer mechanisms were confirmed by photochemical studies performed using

time-resolved emission and femtosecond transient absorption studies in solvents of varying polarity. Ultrafast charge separation has been witnessed in these closely spaced, strongly interacting triads. The charge separated state returned to the ground state without populating the ³BODIPY*.

Keywords: charge separation · BF₂ chelated azadipyromethene · dicyanoquinodimethane · tetracyanobutadiene · triphenylamine

Introduction

The ability to harvest and convert sunlight into chemical energy in the process of photosynthesis has motivated the chemists for the development of artificial photosynthetic systems, which can efficiently absorb and transform sunlight into useful forms of energy to meet the increasing demand for clean and renewable energy sources.^[1–7] A wide variety of artificial photosynthetic model systems have been designed and synthesized mimicking natural photosynthesis, and exhibiting strong absorption in the visible and near-infrared (NIR) regions.^[8] The donor-acceptor (D-A) approach is the most common pathway to design artificial molecular systems as the light harvesting properties can be tuned significantly by altering the D/A units or the π -linker connecting them.^[9,10]

In recent years, BF₂-chelated dipyrromethenes (BODIPY) have gained attention as building blocks of antenna systems and as electron donor or acceptor entities.^[11] BODIPY dyes exhibit high absorption coefficients, high emission quantum yields and tunable redox potentials.^[12] Their photonic properties can be tuned by altering the strength of D/A units or by varying the π -linker at the *meso*-position, as well as at the pyrrolic position.^[12,13] These features make the BODIPY dyes an attractive chromophore, since their absorption can be extended over a wide spectral range. Our groups have explored various antenna-donor-acceptor models possessing substituted BODIPYs in recent years.^[12b, 14]

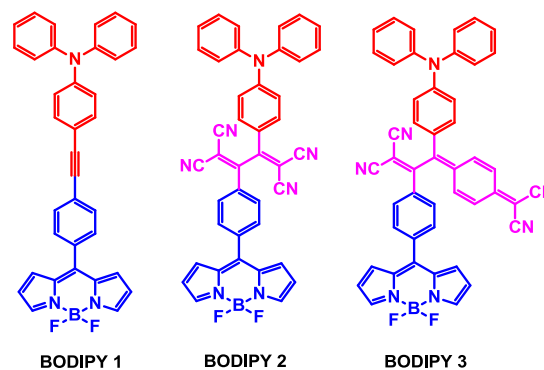


Figure 1. Structure of the BODIPY derived strongly interacting donor acceptor triads.

In continuation of our work in this area of research, in the present study we have synthesized D- π -A dyad, abbreviated as BODIPY **1** in Figure 1 by substitution of the donor triphenylamine (TPA) at the *meso*-position of the BODIPY acceptor via an acetylenic linker. TPA is an electron donor and frequently used for the design of D-A molecular systems.^[15] Next, the acetylene linker of the D- π -A BODIPY **1** was systematically replaced by strong electron acceptor, 1,1,4,4-tetracyanobutadiene (TCBD) and dicyanoquinodimethane (DCNQ) acceptor (BODIPY **2** and BODIPY **3** in Figure 1) to probe the effect of acceptor strength on the photonic properties.^[16] The substitution of the TCBD and DCNQ units have been achieved via [2+2] cycloaddition–retroelectrocyclization of BODIPY **1**, which resulted BODIPYs **2** and **3**. The TCBD and DCNQ substitution resulted in strong intramolecular charge transfer and broadening of the absorption

[a] Department of Chemistry, Indian Institute of Technology, Indore 453552, India. E-mail: rajneeshmisra@iiti.ac.in; Fax: +91 731 2361 482

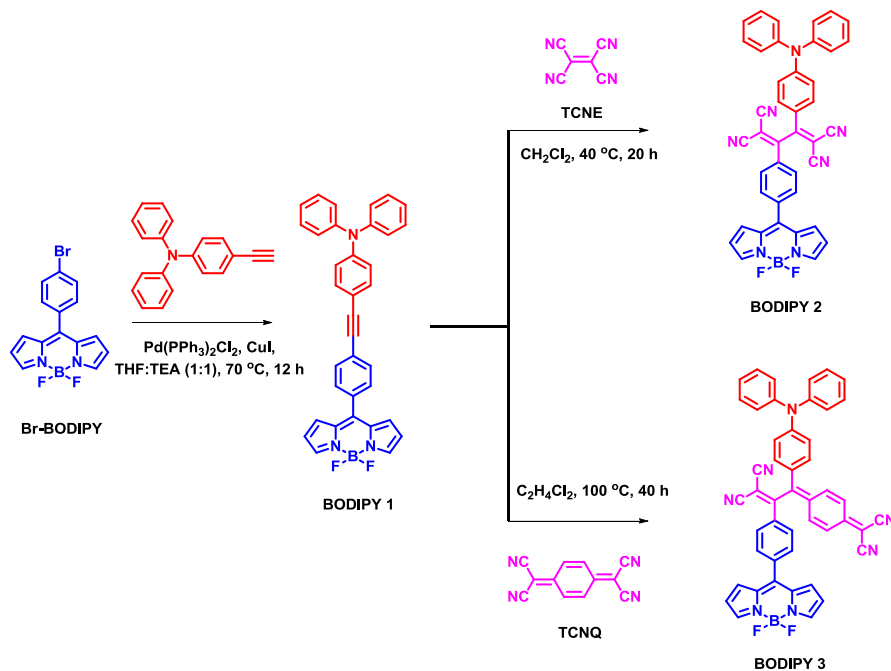
[b] Department of Chemistry, University of North Texas, 1155 Union Circle, #305070, Denton, TX 76203-5017, USA, E-mail: Francis.DSouza@UNT.edu

Supporting information for this article, additional spectral and femtosecond spectra, ¹H and ¹³C NMR and MALDI-mass of triads.

bands. We have explored the photophysical and electrochemical properties of the BODIPYs **1–3** and performed the theoretical calculations to see the effect of enhanced π -conjugation and acceptor strength. Ultrafast charge separation has been witnessed in these triads as revealed by studies involving steady-state and time-resolved emission, and femtosecond transient absorption studies.

Results and Discussion

Syntheses: The synthetic methodology developed for BODIPYs **1–3** donor-acceptor conjugates is shown in Scheme 1. The *meso*-4-bromophenyl-BODIPY (Br-BODIPY) was synthesized in two steps.^[17] The first step involved the reaction of pyrrole and 4-bromobenzaldehyde in the presence of catalytic amounts of trifluoroacetic acid (TFA), resulted in bromo-dipyrrromethane, which upon DDQ oxidation and complexation with $\text{BF}_3 \cdot \text{OEt}_2$, resulted Br-BODIPYs in the final step. The Pd-catalyzed Sonogashira cross-coupling of Br-BODIPY with 4-ethynyl-*N,N*-diphenylamine resulted BODIPY **1** in 74% yield.^[18] The tetracyanobutadiene (TCBD) and dicyanoquinodimethane (DCNQ) substituted BODIPYs **2** and **3** were synthesized by the [2+2] cycloaddition–retroelectrocyclization reaction of the BODIPY **1** with tetracyanoethene (TCNE) and 7,7,8,8-tetracyanoquinodimethane (TCNQ).^[19] The reaction of BODIPY **1** with one equivalent of TCNE and TCNQ resulted BODIPYs **2** and **3** in 75% and 80% yields respectively. The BODIPYs **1–3** were purified by column chromatography and were fully characterized by ^1H , ^{13}C NMR, and HRMS techniques. The BODIPYs **1–3** are readily soluble in common organic solvents such as acetone, chloroform, dichloromethane, toluene, tetrahydrofuran, etc.



Scheme 1. Syntheses of BODIPY derived dyad, **1** and triads **2** and **3**.

Absorbance and fluorescence studies: The electronic absorption spectral studies of the BODIPYs **1–3** were performed in toluene at room temperature and is shown in Figure 2a. The BODIPYs are known to exhibit a strong absorption band around 500 nm along with a broad transition in the higher energy region.^[11, 20] The present TPA functionalized BODIPYs **1–3**

exhibited a strong absorption band between 500–510 nm, corresponding to the $S_0 \rightarrow S_1$ ($\pi \rightarrow \pi^*$) transition, and a weak

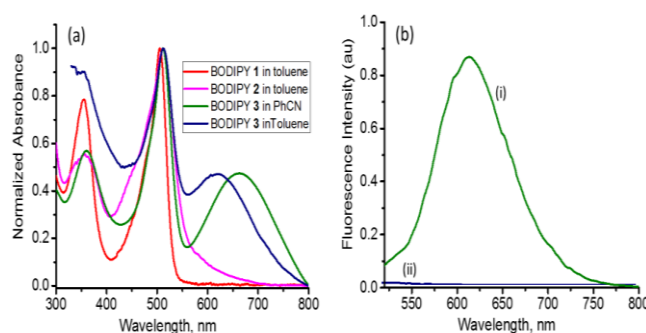


Figure 2. (a) Normalized absorption spectrum of the indicated compounds in toluene, the spectrum of BODIPY **3** in benzonitrile is also shown for comparison purposes. (b) Fluorescence spectrum of BODIPY **1** in (i) toluene ($\lambda_{\text{ex}} = 505$ nm) and (ii) benzonitrile ($\lambda_{\text{ex}} = 507$ nm).

absorption band between 300–400 nm due to the $S_0 \rightarrow S_2$ ($\pi \rightarrow \pi^*$) transition with contributions from the TPA entity. The comparison of the absorption spectra of BODIPYs **1** and **2** indicated that the substitution of TCBD unit results in marginal red-shift of ~ 3 nm but significant broadening of the absorption band due to the $S_0 \rightarrow S_1$ transition. The DCNQ substitute BODIPY **3** exhibited a distinct charge transfer band at 621 nm and a red-shift of ~ 6 nm for the $S_0 \rightarrow S_1$ transition as compared to BODIPY **1**. These results clearly indicate that the electronic absorption of the TPA-substituted BODIPYs is a function of the acceptor strength. As expected for charge transfer bands, changing the solvent to more polar benzonitrile, caused additional red-shift of the charge transfer band to 66 nm, as shown in Figure 2a.^[21]

As shown in Figure 2b(i), the steady state fluorescence spectrum of BODIPY **1** in toluene was found to be located at 61 nm. This peak was significantly red shifted from the fluorescence of pristine BODIPY derivatives known to emit in the 520 nm range. This observation suggests electronic coupling between the TPA and BODIPY entities via the acetylenic linker resulting into intramolecular excimer emission in nonpolar solvent. Changing the solvent to a more polar benzonitrile quenched the fluorescence quantitatively (Figure 2b(ii)) revealing complete electrotransfer from the singlet excited BODIPY to TPA.^[22] As expected for strongly coupled donor-acceptor systems, no measurable fluorescence was observed for BODIPY **2** and BODIPY **3** in both nonpolar and polar solvents. Fluorescence lifetime of BODIPY **1** was measured in toluene using time-correlated single photon counting (TCSPC) method using 495 nm nanoLED excitation source. The decay was monoexponential with the lifetime of 2.24 ns (see Figure S1 in SI for decay curve).

Electrochemical properties: The electrochemical properties of the BODIPYs **1–3** were explored by cyclic voltammetry (CV) and differential pulse voltammetry (DPV). All the measurements were performed in benzonitrile at room temperature using tetrabutylammonium perchlorate, (TBA)ClO₄, as a supporting electrolyte. The electrochemical data are listed in Table 1, and the representative cyclic voltammograms are shown in Figure 3. BODIPY **1** revealed the first reduction at -0.68 V vs. Ag/AgCl corresponding to BODIPY^{0/•-} formation. In addition, two oxidation processes, the first one a quasi-reversible process at $E_{pa} = 1.07$ corresponding to oxidation of TPA entity and the second one at $E_{pa} = 1.71$ V corresponding to oxidation of BODIPY entity were observed. Interestingly, for BODIPY **2** and BODIPY **3**, in addition to the expected reduction and oxidation processes of BODIPY and TPA, additional reduction processes were observed corresponding to the reduction of TCBD and DCNQ entities. For BODIPY **2**, two one-electron reductions corresponding to TCBD^{0/•-} and TCBD^{•-/2-} were observed at -0.56 and -0.20 V, respectively. Similarly, for BODIPY **3**, two one-electron reductions corresponding to DCNQ^{0/•-} and DCNQ^{•-/2-} were observed at -0.18 and -0.05 V, respectively. It is important to note that the first reduction potential corresponding to TCBD in BODIPY **2** and DCNQ in BODIPY **3** was lower than that reported for traditional electron acceptors like quinone or fullerene.^[23] The BODIPY reduction in BODIPY **2** and BODIPY **3** were cathodically shifted and appeared at -0.91 and -0.78 V, respectively, owing to the presence of reduced TCBD and DCNQ entities prior to the reduction of BODIPY. Such a trend in oxidation potentials was also observed. In the case of BODIPY **2**, the oxidation processes corresponding to TPA and BODIPY were located at $E_{pa} = 1.36$ and 1.71 V while in the case of BODIPY **3**, these processes were located at $E_{pa} = 1.09$ and 1.72 V. The harder oxidations are due to the electronic effects caused by the strong electron acceptor entities directly located between the BODIPY and TPA entities (see Figure 1 for structures).

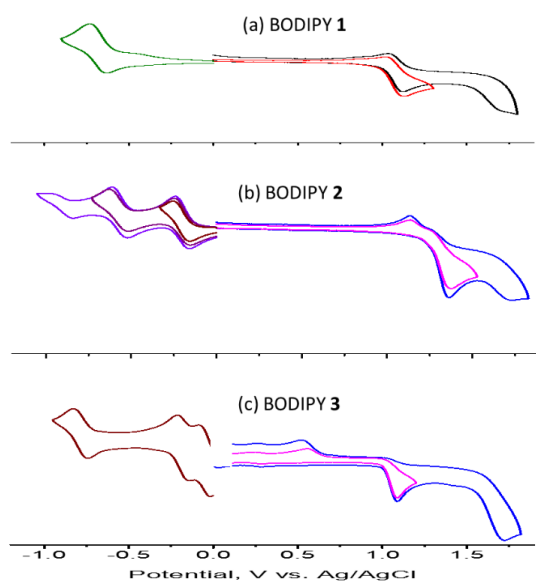


Figure 3. Cyclic voltammogram of triphenylamine functionalized BODIPYs **1–3** in 0.1M (TBA)ClO₄ in benzonitrile recorded at a scan rate of 100 mV s⁻¹.

Table 1. Redox potential corresponding to both oxidation and reduction processes in benzonitrile, 0.1 M (TBA)ClO₄ (V vs. Ag/AgCl) and free-energy change for charge recombination and charge separation from ¹BODIPY* of BODIPY **1–3**. The site of electron transfer corresponding to each redox couple is listed in the table footnote.

Compound	3 rd red, V	2 nd red, V	1 st red, V	1 st ox	2 nd ox	ΔG_{CR}^f , eV	ΔG_{CS}^i , eV
BODIPY 1	-0.68 ^a	--	--	1.07 ^b	1.71 ^{a,e}	-1.74 ^g	-0.59 ^g
BODIPY 2	-0.91 ^a	-0.56 ^c	-0.20 ^c	1.36 ^{b,e}	1.71 ^{a,e}	-1.49 ^h	-0.84 ^h
BODIPY 3	-0.78 ^a	-0.18 ^d	-0.05 ^d	1.09 ^{b,e}	1.72 ^{a,e}	-1.14 ^h	-1.19 ^h
						-1.53 ⁱ	-0.80 ⁱ

^a-BODIPY centered oxidation and reduction processes

^b-TPA centered oxidation

^c-TCBD centered reductions

^d-DCNQ centered reductions

^e- E_{pa} at scan rate = 0.1 V/s

^f-calculated using equation 1

^g-for BODIPY^{•-}-TPA^{•+}

^h-for BODIPY-Acceptor^{•-}-TPA^{•+} (Acceptor = TCBD or DCNQ)

ⁱ-for BODIPY^{•-}-Acceptor^{•-}-TPA (Acceptor = TCBD or DCNQ)

^j-from ¹BODIPY* ($E_{0,0} = 2.33$ eV, mid-point of absorption and emission peak maxima).

Computational Studies: In order to explore the geometry and electronic structures of triphenylamine functionalized BODIPYs, DFT (density functional theory) calculations were performed at the B3LYP/6-31G+g(d) level in the gas phase.^[24] The structures were fully optimized on a Born-Oppenheimer potential energy surface and establishment of true minima was confirmed by frequency calculations. No steric constraints between the centrally located electron acceptor, TCBD or DCNQ, with the BODIPY or TPA entities were observed. The contours of the HOMOs and LUMOs of the optimized structures of BODIPYs **1–3** along with the electrostatic potential map is shown in Figure 4 while high energy LUMOs are shown in Figures S2 and S3. In all the structures, the HOMO-1 was found to be localized over the BODIPY segment while HOMO was delocalized mainly over the triphenylamine donor entity with some contributions on π -extended central entities. The

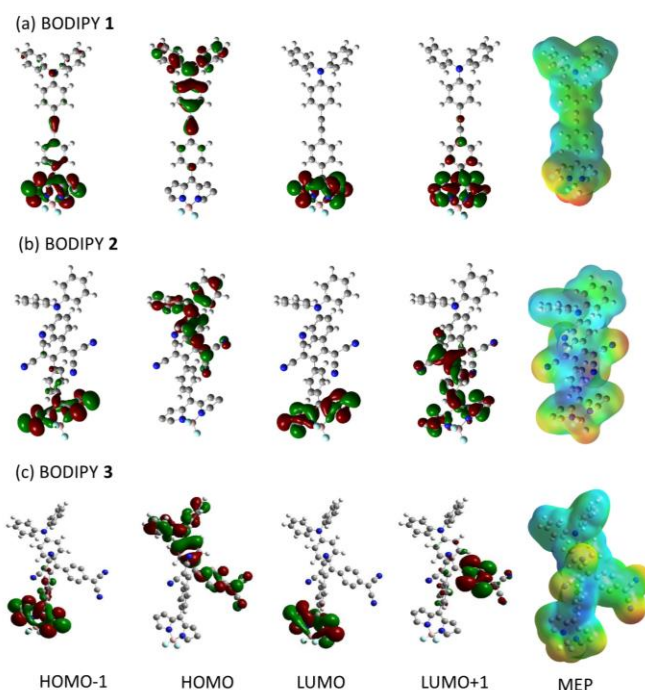


Figure 4. Frontier molecular orbitals and electrostatic potential map of triphenylamine functionalized BODIPYs **1–3**.

LUMO was found to be localized mainly over BODIPY while LUMO+1 on the TCBD and DCNQ acceptor entities in the case of **2** and **3**. The LUMO on BODIPY and LUMO+1 on TCBD or DCNQ due to level of calculations done in gas phase. The electrostatic potential maps were consistent with the electron rich (TPA) and deficient parts (TCBD and DCNQ) of the studied systems.

The orbital location is helpful in arriving the electron transfer path. For example, in BODIPY **1**, the initial excitation of BODIPY involves HOMO-1 to LUMO. For charge separation to occur, one of the two electron on the HOMO located on TPA drops to the half-filled HOMO-1, giving rise to BODIPY⁻-TPA⁺ charge separated state. In addition, the ground state charge transfer band observed in the case of BODIPY **3** (see Fig. 2a) corresponds to the transition from the HOMO to LUMO+1 transition, resulting in a partial charge transfer from TPA to DCNQ without much contribution from BODIPY centered transition involving HOMO-1 and LUMO. This is conceivable since the oxidation of TPA entity is much more facile than BODIPY in these molecular systems (see Table 1) making the charge transfer interactions between TPA-DCNQ much stronger than BODIPY-DCNQ.

Free-energy calculations and energy level diagram: Using the spectral, computational and electrochemical data, Gibbs free-energy change associated for charge recombination and charge separation were estimated according to equations 1-3 [25]

$$-\Delta G_{CR} = E_{ox} - E_{red} + \Delta G_s \quad (i)$$

$$-\Delta G_{CS} = \Delta E_{00} - (-\Delta G_{CR}) \quad (ii)$$

where ΔE_{00} corresponds to the energy of ¹BODIPY* (= 2.33 eV, mid-point of absorption and emission peak maxima). The term ΔG_s refers to electrostatic energy calculated according to dielectric continuum model (see equation iii). The E_{ox} and E_{red} represent the oxidation potential of the electron donor (TPA or BODIPY) and the first reduction potential of the electron acceptor (BODIPY in the case of **1**, TCBD in the case of **2** and DCNQ in the case of **3**), respectively.

$$\Delta G_s = \frac{e^2}{4\pi\epsilon_0} \left[\left(\frac{1}{2R_+} + \frac{1}{2R_-} \right) \Delta \left(\frac{1}{\epsilon_r} \right) - \frac{1}{R_{CC}\epsilon_r} \right] \quad (iii)$$

The symbols ϵ_0 and ϵ_r represent vacuum permittivity and dielectric constant of the solvent used for photochemical and electrochemical studies, respectively. The symbols R_+ and R_- represent radii of the cation and anion, respectively. R_{CC} are the center-to-center distances between donor and acceptor entities of the dyad from the computed structures in Figure 4.

The ΔG_{CR} and ΔG_{CS} values estimated using the above procedure are given in Table 1. The following observations were made. (i) In the case of BODIPY **1**, the only thermodynamically possible charge separated state from ¹BODIPY* is BODIPY⁻-TPA⁺ due to facile oxidation of TPA over BODIPY. In the case of BODIPY **2** and BODIPY **3**, at least two charge separated states were possible, viz., BODIPY⁺-Acceptor⁻-TPA and BODIPY-Acceptor⁻-TPA⁺ (Acceptor = TCBD or DCNQ). At the excitation wavelength of 400 nm (operating wavelength of our femtosecond transient spectrometer), it is possible that part of TPA might be directly excited to yield BODIPY-Acceptor⁻-TPA⁺ charge separated state. Although not discussed in detail, such processes are also thermodynamically feasible.

The relative energy levels of the charge separated states with respect to the energy of the singlet and triplet excited BODIPY in

the case of BODIPY **2** and BODIPY **3** is shown in Figure 5. The solid arrows show the major process while the dashed arrows show minor process. In these compounds ¹BODIPY* could undergo intersystem crossing to populate the ³BODIPY* state in competition with electron transfer to result in charge separated states. Due to close distance and exothermic nature, electron transfer might prevail over the intersystem crossing process. The charge recombination process also deserves special mention. Similar to the charge separation process, the charge recombination process could also be predicted to occur faster due to close distal separation and lack of molecular entities causing additional electron or hole transfer processes. In addition, among all of the charge separated states, only BODIPY⁻-TCBD⁻-TPA possess energy higher than that of ³BODIPY*. In such a case, the charge separated state could populate the ³BODIPY* prior returning to the ground state. In order to unravel these mechanistic aspects, femtosecond transient absorption studies were performed as discussed in the following section.

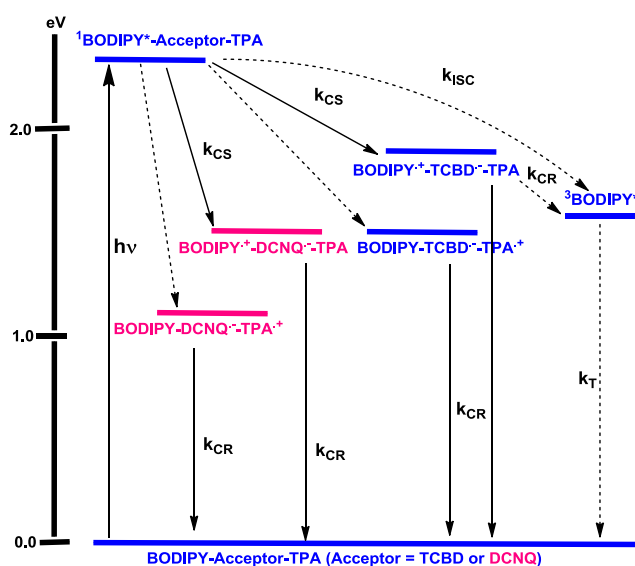


Figure 5. Energy level diagram showing the different photochemical event occurring in BODIPY **2** and BODIPY **3** benzonitrile. Energies of different states were evaluated from spectral and electrochemical studies. Solid arrows indicate major photo-processes, dashed arrow indicates minor photo-process. ISC – intersystem crossing, CS = charge separation, CR = charge recombination, and T = emission from triplet excited state.

Femtosecond transient absorption studies: Since strong excited state charge transfer type interactions in the studied system especially in BODIPY **2** and BODIPY **3** were expected femtosecond transient absorption studies were performed in solvent of varying polarity. Four solvents, toluene, tetrahydrofuran (THF), benzonitrile (PhCN) and dimethylformamide (DMF) were employed. The samples were excited at 400 nm where BODIPY was mainly excited and to a lesser extent TPA was also excited. Figures 6 and 7 show representative spectral features at different delay times in toluene and benzonitrile while Figures S2 and S3 in SI show the data in THF and DMF. Additional time profiles are shown in Figures S7-S9. Steady-state fluorescence studies revealed quantitative quenching of all three BODIPY derivatives in both polar and nonpolar solvents except in the case of BODIPY **1** in toluene. Figure 6a shows the transient absorption spectra of BODIPY **1** in toluene at the indicated delay time. The instantaneously formed ¹BODIPY* revealed peak at 508 nm due to ground state depletion, and positive peaks at 461 and 540 nm along

with a broad peak in the near-infrared region at 1200 nm. These peaks have been assigned to the exciplex state. Figure 6a right hand panel shows the time profiles of the 508 and 1200 nm peaks. Slower recovery of the 508 nm peak and slower decay of the 1200 nm are consistent with the longer lifetime of the exciplex state of BODIPY 1 (2.24 ns) discussed earlier.

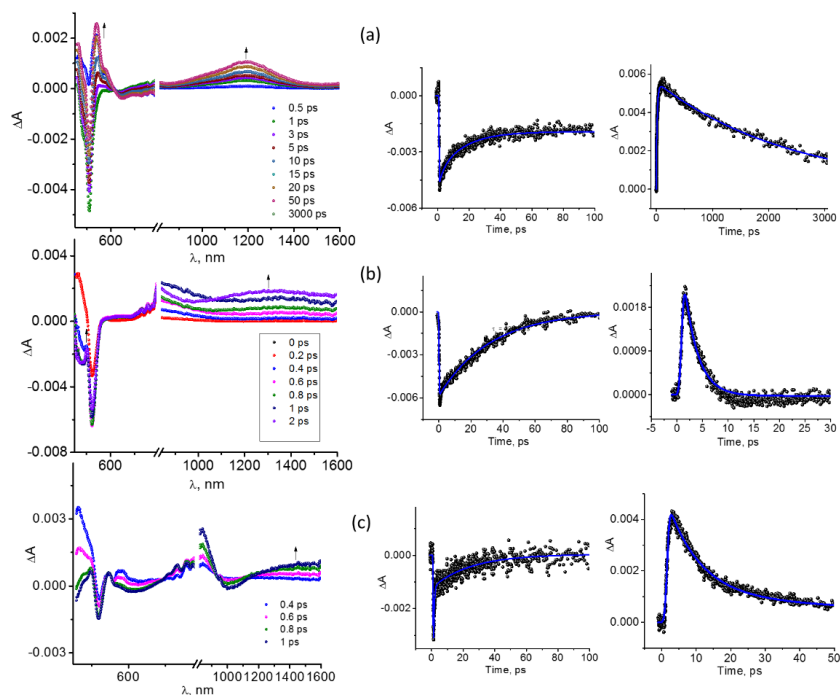


Figure 6. Femtosecond transient spectra at the indicated delay times of (a) BODIPY 1, (b) BODIPY 2 and (c) BODIPY 3 in Ar-saturated toluene (400 nm, 100 fs pulses). Time profiles of the ground state bleaching peak in the 520 nm range, and rise and decay of the near-IR peak is shown at the right hand side of each figure.

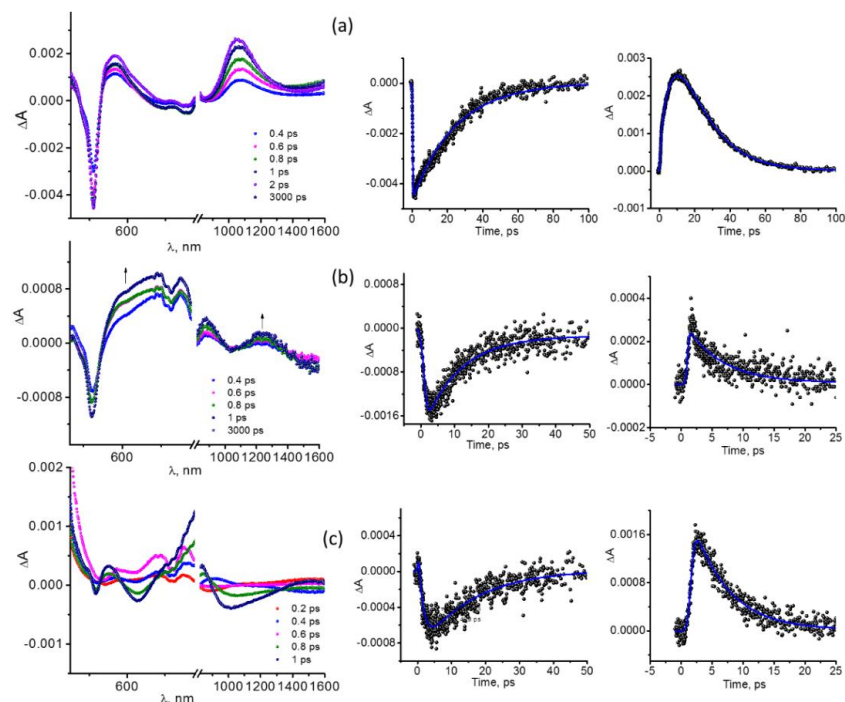


Figure 7. Femtosecond transient spectra at the indicated delay times of (a) BODIPY 1, (b) BODIPY 2 and (c) BODIPY 3 in Ar-saturated benzonitrile (400 nm, 100 fs pulses). Time profiles of the ground state bleaching peak in

the 520 nm range, and rise and decay of the near-IR peak is shown at the right hand side of each figure.

In sharp contrast, both BODIPY 2 (Figure 6b) and BODIPY 3 (Figure 6c) revealed ultrafast photochemical events. In the case of BODIPY 2, the instantly formed $^1\text{BODIPY}^*$ revealed a positive peak at 465 nm and depleted peak at 522 nm due to ground state bleaching. Decay and recovery of these peaks were fast that revealed new peaks at 501 and 1350 nm that has been assigned to the formation of $\text{BODIPY}^{+-}\text{TCBD}^-\text{TPA}$ charge separated state with additional contributions from the $\text{BODIPY-TCBD}^-\text{TPA}^{++}$ charge separated state. Decay of the charge separated signals was also rapid as shown in Figure 6b right hand side panel meaning ultrafast charge recombination. In the case of BODIPY 3, the instantaneously formed $^1\text{BODIPY}^*$ revealed positive peaks at 465 and 84 nm and negative peaks at 518 and 620 nm. These transient peaks have been attributed to $\text{BODIPY}^{+-}\text{DCNQ}^-\text{TPA}$ and $\text{BODIPY-DCNQ}^-\text{TPA}^{++}$ charge separated states.

Changing the solvent to more polar solvent would facilitate the charge separation process, this indeed seems to be the case as shown in the transient spectra of the investigated compounds in benzonitrile in Figure 7 (see Figures S2 and S3 for transient spectra in THF and DMF). In the case of BODIPY 1 in PhCN, instantly formed $^1\text{BODIPY}^*$ revealed positive peaks at 566 and 1055 nm corresponding to TPA^{++} and BODIPY^{+-} , respectively (Figure 7c) implying occurrence of excited state electron transfer. The formation and decay of these signals were much faster than those observed in toluene, consistent with higher degree of quenching observed for BODIPY 1 in benzonitrile (see time profiles at the

right hand panels). In the case of BODIPY 2 and BODIPY 3, the spectral features were similar to that observed in toluene, however, with shorter time constants for both growth and decay of the signals, predicted for charge transfer interactions. The spectral features were attributable to $\text{BODIPY}^{+-}\text{TCBD}^-\text{TPA}$ and $\text{BODIPY-TCBD}^-\text{TPA}^{++}$ charge separated states in the case of BODIPY 2, and $\text{BODIPY}^{+-}\text{DCNQ}^-\text{TPA}$ and $\text{BODIPY-DCNQ}^-\text{TPA}^{++}$ charge separated states in the case of BODIPY 3. The time constants for the growth and decay of the signals from global analysis for the transient spectral data is given in Table 2.

From the data presented in Table 2 it is clear that ultrafast charge separation and recombination processes occur especially in BODIPY 2 and BODIPY 3. In some cases the τ_{CS} are within the time resolution of the transient setup. To a large extent, both τ_{CS} and τ_{CR} follow the expected solvent polarity trend. The very close proximity of BODIPY to the strong electron acceptors, TCBD or DCNQ made such processes possible.

Table 2. Time constants for photoinduced charge separation, τ_{CS} and charge recombination, τ_{CR} of the investigated donor-acceptor systems in solvents of varying polarity (estimated error = $\pm 10\%$).

Compound	Solvent	Dielectric constant	τ_{CS} , ps	τ_{CR} , ps
BODIPY 1	Toluene	2.38	18.4	2420
	THF	7.58	3.73	64.5
	PhCN	26.0	1.72	7.80
	DMF	36.7	2.49	4.0
BODIPY 2	Toluene	2.38	1.50	2.65
	THF	7.58	1.12	2.74
	PhCN	26.0	1.55	5.86
	DMF	36.7	< 1ps	4.94
BODIPY 3	Toluene	2.38	9.60	104
	THF	7.58	< 1 ps	1.59
	PhCN	26.0	< 1 ps	5.72
	DMF	36.7	< 1 ps	1.54

Conclusion

In summary, triphenylamine functionalized donor-acceptor BODIPYs **1–3** were newly synthesized to explore the effect of substitution of the highly electron deficient tetracyanobutadiene (TCBD) and dicyanoquinodimethane (DCNQ) acceptor units on their physico-chemical properties. The synthesis involving Pd-catalysed Sonogashira cross-coupling and [2+2] cycloaddition-retroelectrocyclization reactions resulted in good yields. The absorption studies showed strong intramolecular charge transfer and bathochromic shift of the absorption bands upon increasing the acceptor strength. The electron acceptor properties of the centrally positioned DCNQ and TCBD in the BODIPY-TPA systems revealed reversible reductions whose potentials were lower than the traditional electron acceptors. Due to this strong electron acceptor behavior and close proximity between the donor and acceptor entities, strong intramolecular type interactions both in the ground and excited state were observed. Excited state charge transfer from singlet excited BODIPY and TPA to the electron to the electron acceptors was established from femtosecond transient absorption studies in solvents of varying polarity. Ultrafast kinetic events were witnessed in the present series of compounds highlighting their importance in solar energy harvesting and optoelectronic applications.

Experimental Section

Chemicals. All the reagents were from Aldrich Chemicals (Milwaukee, WI) while the bulk solvents utilized in the syntheses were from Fischer Chemicals. The tetra-*n*-butylammonium perchlorate (TBA)ClO₄ used in electrochemical studies was from Fluka Chemicals.

Syntheses

BODIPY 1. To a stirred solution of Br-BODIPY (347 mg; 1 mmol) and 4-ethynyl-*N,N*-diphenylamine (296 mg; 1.1 mmol) in THF and TEA (1:1, v/v) were added [PdCl₂(PPh₃)₂] (50 mg, 0.07 mmol) and CuI (10 mg, 0.05 mmol) at room temperature under an argon flow. The reaction mixture was stirred for 12 h at 70 °C, and then cooled to room temperature. The solvent was evaporated under reduced pressure, and the mixture was purified by SiO₂ chromatography with DCM/hexane (1:1, v/v), to obtain BODIPY **1** as red colored solids (396 mg, Yield: 74 %); ¹H NMR (400 MHz, δ in ppm): 7.95 (s, 2H), 7.65 (d, 2H, *J* = 8 Hz), 7.55 (d, 2H, *J* = 8 Hz), 7.40 (d, 2H, *J* = 8 Hz), 7.31-7.27 (m, 4H), 7.14-7.08 (m, 6H), 7.02 (d, 2H, *J* = 8 Hz), 6.96 (d, 2H, *J* = 4 Hz), 6.57 (d, 2H, *J* = 4 Hz); ¹³C NMR (100 MHz, CDCl₃, δ in ppm): 148.5, 147.1, 144.2, 139.3, 134.7, 133.1, 132.8, 131.4, 130.6, 129.5, 126.7, 125.2,

123.8, 122.0, 118.7, 115.2, 114.1, 93.0, 87.7; HRMS (ESI-TOF) *m/z* calcd for C₃₅H₂₄BF₂N₃ + Na: 558.1930 [M + Na]⁺, found 558.1931 [M + Na]⁺.

BODIPY 2. TCNE (26 mg, 0.20 mmol) was added to a solution of BODIPY **1** (107 mg; 0.20 mmol) in DCM (50 mL). The mixture was refluxed at 40 °C for 20 h. The solvent was removed in vacuo, and the product was purified by SiO₂ column chromatography with DCM as the eluent to yield BODIPY **2** as brown colored solid (100 mg, Yield: 75 %); ¹H NMR (400 MHz, CDCl₃, δ in ppm): 7.99 (s, 2H), 7.87 (d, 2H, *J* = 8 Hz), 7.75-7.71 (m, 4H), 7.43 (t, 4H), 7.31-7.24 (m, 3H), 7.24 (bs, 3H), 6.98 (d, 2H, *J* = 8 Hz), 6.88 (d, 2H, *J* = 4 Hz), 6.59 (d, 2H, *J* = 4 Hz); ¹³C NMR (100 MHz, CDCl₃, δ in ppm): 167.5, 162.9, 154.3, 145.6, 144.4, 139.5, 134.6, 133.6, 132.1, 131.6, 131.5, 130.3, 129.5, 127.2, 121.0, 119.5, 118.2, 113.5, 113.0, 111.7, 111.0, 89.2, 77.8; HRMS (ESI-TOF) *m/z* calcd for C₄₁H₂₄BF₂N₇ + Na: 686.2053 [M + Na]⁺, found 686.2054 [M + Na]⁺.

BODIPY 3. TCNQ (41 mg, 0.20 mmol) was added to a solution of BODIPY **1** (107 mg; 0.20 mmol) in DCE (50 mL). The mixture was refluxed at 100 °C for 40 h. The solvent was removed in vacuo, and the product was purified by SiO₂ column chromatography with DCM as the eluent to yield BODIPY **3** black colored solid (115 mg, Yield: 80 %); ¹H NMR (400 MHz, CDCl₃, δ in ppm): 7.99 (s, 2H), 7.81 (d, 2H, *J* = 8 Hz), 7.69 (d, 2H, *J* = 8 Hz), 7.56-7.52 (m, 1H), 7.40-7.32 (m, 5H), 7.25-7.19 (m, 9H), 7.06-6.99 (m, 3H), 6.84 (d, 2H, *J* = 4 Hz), 6.59 (bs, 2H); ¹³C NMR (100 MHz, CDCl₃, δ in ppm): 170.153.7, 151.7, 149.3, 145.4, 145.2, 144.0, 138.6, 136.2, 135.1, 134.5, 133.133.1, 131.4, 131.2, 130.0, 129.5, 126.6, 126.5, 126.3, 126.1, 119.3, 113.112.5, 111.8, 88.9, 75.4; HRMS (ESI-TOF) *m/z* calcd for C₄₇H₂₈BF₂N₇ + N 762.2367 [M + Na]⁺, found 762.2365 [M + Na]⁺.

Instruments: The UV-visible spectral measurements were carried out with Shimadzu Model 2550 double monochromator UV-visible spectrophotometer. The fluorescence emission was monitored by using a Horiba Yvon Nanok coupled with time-correlated single photon counting with nanoLE excitation sources. A right angle detection method was used. Different pulse and cyclic voltammograms were recorded on an EG&G PARSTAT electrochemical analyzer using a three electrode system. A platinum butt electrode was used as the working electrode. A platinum wire served as the counter electrode and an Ag/AgCl electrode was used as the reference electrode. Ferrocene/ferrocenium redox couple was used as an internal standard. All the solutions were purged prior to electrochemical and spectral measurements using argon gas. The computational calculations were performed with the use of GAUSSIAN 09 software package [24]. All the oxygen or moisture sensitive reactions were carried out under argon/nitrogen atmosphere. ¹H NMR spectra were recorded using a 400 MHz spectrometer. Chemical shifts are reported in delta (δ) units, expressed in parts per million (ppm) downfield from tetramethylsilane using residual protonated solvent as an internal standard {CDCl₃, 7.26 ppm}. ¹³C NMR spectra were recorded using a 100 MHz spectrometer. Chemical shifts are reported in delta (δ) unit expressed in parts per million (ppm) downfield from tetramethylsilane using the solvent as internal standard {CDCl₃, 77.0 ppm}. The ¹H NMR splitting patterns have been described as “s, singlet; d, doublet; t, triplet and r multiplet”. HRMS was recorded on TOF-Q mass spectrometer.

Femtosecond pump-probe transient spectroscopy. Femtosecond transient absorption spectroscopy experiments were performed using an Ultrafast Femtosecond Laser Source (Libra) by Coherent incorporating diode-pumped mode locked Ti:Sapphire laser (Vitesse) and diode-pumped intra cavity doubled Nd:YLF laser (Evolution) to generate a compressed laser output of 1.45 W. For optical detection, a Helios transient absorption spectrometer coupled with femtosecond harmonics generator both provided by Ultrafast Systems LLC was used. The source for the pump and probe pulses were derived from the fundamental output of Libra (Compressed output 1.45 W, pulse width 100 fs) at a repetition rate of 1 kHz. 95% of the fundamental output of the laser was introduced into harmonic generator, which produces second and third harmonics of 400 and 267 nm besides the fundamental 800 nm for excitation, while the rest of the output was used for generation of white light continuum. In the present study, the second harmonic 400 nm excitation pump was used in all the experiments. Kinetic traces at appropriate wavelengths were assembled from the time-resolved spectral data. Data

analysis was performed using Surface Explorer software supplied by Ultrafast Systems. All measurements were conducted in degassed solutions at 298 K.

Acknowledgments

Support by the US-National Science Foundation (grant no. 1401188 to FD) is acknowledged.

- [1] a) J. Deisenhofer, O. Epp, K. Miki, R. Huber, H. Michel, *J. Mol. Biol.* **1984**, *180*, 385; b) C. Kirmaier, D. Holton in *The Photosynthetic Reaction Center*, Vol II (Eds.: J. Deisenhofer, J. R. Norris), Academic Press, San Diego, 1993, pp. 49–70; c) *The Photosynthetic Reaction Center* (Eds.: J. Deisenhofer, J. R. Norris), Academic Press, San Diego, 1993; d) R. E. Blankenship, *Molecular Mechanisms of Photosynthesis*, Blackwell Sciences, Oxford, 2002; e) *Photosynthetic Light Harvesting* (Eds.: R. Cogdell, C. Mullineaux), Springer, Dordrecht, 2008. f) *Handbook of Photosynthesis*, 2nd ed. (Ed.: M. Pessaraki), CRC, Boca Raton, 2005;
- [2] a) M. R. Wasielewski, *Acc. Chem. Res.* **2009**, *42*, 1910. b) M. R. Wasielewski, *Chem. Rev.* **1992**, *92*, 435; c) D. Gust, T. A. Moore, A. L. Moore, *Acc. Chem. Res.* **2001**, *34*, 40; d) D. Gust, T. A. Moore, A. L. Moore, *Acc. Chem. Res.* **2009**, *42*, 1890.
- [3] a) N. Armaroli, V. Balzani, *Angew. Chem.* **2007**, *119*, 52; *Angew. Chem. Int. Ed.* **2007**, *46*, 52. b) A. Harriman, J. P. Sauvage, *Chem. Soc. Rev.* **1996**, *25*, 41; c) V. Balzani, A. Juris, M. Venturi, S. Campagna, S. Serroni, *Chem. Rev.* **1996**, *96*, 759; d) M. J. Blanco, M. C. Jiménez, J. C. Chambron, V. Heitz, M. Linke, J. P. Sauvage, *Chem. Soc. Rev.* **1999**, *28*, 293.
- [4] a) L. Sánchez, M. Nazario, D. M. Guldi, *Angew. Chem.* **2005**, *117*, 5508; *Angew. Chem. Int. Ed.* **2005**, *44*, 5374; b) D. M. Guldi, *Chem. Commun.* **2000**, 321; c) A. Mateo-Alonso, D. M. Guldi, F. Paolucci, M. Prato, *Angew. Chem.* **2007**, *119*, 8266; *Angew. Chem. Int. Ed.* **2007**, *46*, 8120; d) D. M. Guldi, *Phys. Chem. Chem. Phys.* **2007**, *9*, 1400; e) V. Sgobba, D. M. Guldi, *Chem. Soc. Rev.* **2009**, *38*, 165.
- [5] a) H. Imahori, S. Fukuzumi, *Adv. Funct. Mater.* **2004**, *14*, 525; b) S. Fukuzumi, *Phys. Chem. Chem. Phys.* **2008**, *10*, 2283; c) G. de La Torre, G. Christian, T. Torres, *Chem. Commun.* **2007**, 2000; d) S. Fukuzumi, *Pure Appl. Chem.* **2007**, *79*, 981; e) S. Fukuzumi, T. Kojima, *J. Mater. Chem.* **2008**, *18*, 1427.
- [6] a) R. Chitta, F. D'Souza, *J. Mater. Chem.* **2008**, *18*, 1440; b) F. D'Souza, O. Ito in *Handbook of Organic Electronics and Photonics*, Vol 1 (Ed.: H. S. Nalwa), American Scientific, Los Angeles, 2008, Chapter 13, pp. 485–521; c) F. D'Souza, A. S. D. Sandanayaka, O. Ito, *J. Phys. Chem. Lett.* **2010**, *1*, 2586. d) O. Ito, F. D'Souza, *Molecules*, **2012**, *17*, 5816-5835.
- [7] a) J. S. Sessler, B. Wang, S. L. Springs, C. T. Brown in *Comprehensive Supramolecular Chemistry* (Eds.: J. L. Atwood, J. E. D. Davies, D. D. MacNicol, F. Vçgtle), Pergamon, New York, 1996, Chapter 9; b) J. L. Sessler, C. M. Lawrence, J. Jayawickramarajah, *Chem. Soc. Rev.* **2007**, *36*, 314.
- [8] a) *The Porphyrin Handbook*; Kadish, K. M., Smith, K. M., Guillard, R., Eds.; Academic Press: San Diego, CA, 2000; Vols. 1–20. b) *Phthalocyanine: Properties and Applications*; Leznoff, C. C., Lever, A. B. P., Eds.; VCH: New York, 1993. c) Claessens, C. G.; González-Rodríguez, D.; Torres, T. *Chem. Rev.* **2002**, *102*, 835–853. d) Kobayashi, N. *Bull. Chem. Soc. Jpn.* **2002**, *75*, 1–19. e) Saito, S.; Osuka, A. *Angew. Chem., Int. Ed.* **2011**, *50*, 4342–4373. f) Mack, J.; Kobayashi, N. *Chem. Rev.* **2011**, *111*, 281–321. g) Claessens, C. G.; Gonzalez-Rodríguez, D.; Rodriguez-Morgade, M. S.; Medina, A.; Torres, T. *Chem. Rev.* **2014**, *114*, 2192–2277.
- [9] a) Wasielewski, M. R. *Acc. Chem. Res.* **2009**, *42*, 1910–1921. b) Gust, D.; Moore, T. A.; Moore, A. L. *Acc. Chem. Res.* **2001**, *34*, 40–48. c) Gust, D.; Moore, T. A.; Moore, A. L. *Acc. Chem. Res.* **2009**, *42*, 1890–1898. d) Bottari, G.; de la Torre, G.; Guldi, D. M.; Torres, T. *Chem. Rev.* **2010**, *110*, 6768–6816. e) F. D'Souza, O. Ito, *Chem. Soc. Rev.* **2012**, *41*, 86–96.
- [10] a) Wang, J.-L.; Xiao, Q.; Pei, J. *Org. Lett.* **2010**, *12*, 4164–4167. b) Zhang, H.; Wan, X.; Xue, X.; Li, Y.; Yu, A.; Chen, Y. *Eur. J. Org. Chem.* **2010**, 1681–1687. c) Bures, F.; Schweizer, W. B.; May, J. C.; Boudon, C.; Gisselbrecht, J.-P.; Gross, M.; Biaggio, I.; Diederich, F. *Chem.—Eur. J.* **2007**, *13*, 5378–5387.
- [11] a) F. D'Souza, P. M. Smith, M. E. Zandler, A. L. McCarty, M. Itou, Y. Araki, O. Ito, *J. Am. Chem. Soc.* **2004**, *126*, 7898; b) J.-Y. Liu, H.-S. Yeung, W. Xu, X. Li, D. K. P. Ng, *Org. Lett.* **2008**, *10*, 5421; c) E. A. Ermilov, J.-Y. Liu, D. K. P. Ng, B. Rçder, *Phys. Chem. Chem. Phys.* **2009**, *11*, 6430; d) J.-Y. Liu, E. A. Ermilov, B. Rçder, D. K. P. Ng, *Chem. Commun.* **2009**, 1517; e) H. Imahori, H. Norieda, H. Yamada, N. Nishimura, I. Yamazaki, Y. Sakata, S. Fukuzumi, *J. Am. Chem. Soc.* **2001**, *123*, 100; f) E. Maligaspe, N. V. Tkachenko, N. K. Subbaiyan, R. Chitta, M. E. Zandler, H. Lemmetyinen, F. D'Souza, *J. Phys. Chem. A* **2009**, *113*, 8478; g) E. Maligaspe, T. Kumpulainen, N. K. Subbaiyan, M. E. Zandler, H. Lemmetyinen, N. V. Tkachenko, F. D'Souza, *Phys. Chem. Chem. Phys.* **2010**, *12*, 7434. h) S. Hattori, K. Ohkubo, Y. Urano, H. Sunahara, T. Nagano, Y. Wada, N. V. Tkachenko, H. Lemmetyinen, S. Fukuzumi, *J. Phys. Chem. B* **2005**, *109*, 15368; i) T. Matsumoto, Y. Urano, T. Shoda, H. Kojima, T. Nagano, *Org. Lett.* **2007**, *9*, 3375; j) R. Ziessel, P. Retailleau, K. J. Elliott, A. Harriman, *Chem. Eur. J.* **2009**, *15*, 10369. k) T. Rousseau, A. Cravino, E. Ripaud, P. Leriche, S. Rihn, A. De Nicola, R. Ziessel, J. Roncali, *Chem. Commun.* **2010**, *46*, 5082; l) T. Rousseau, A. Cravino, T. Bura, G. Ulrich, R. Ziessel, J. Roncali, *J. Mater. Chem.* **2009**, *19*, 2298. m) S. Shao, H. B. Gobeze, P. A. Karr, F. D'Souza, *Chem. Eur. J.* **2015**, *21*, 16005–16016.
- [12] a) Loudet, A.; Burgess, K. *Chem. Rev.* **2007**, *107*, 4891–4932. b) I[†] Khoully, M. E.; Fukuzumi, S.; D'Souza, F. *ChemPhysChem* **2014**, *15*, 30–47.
- [13] a) Umezawa, K.; Nakamura, H.; Makino, D.; Citterio, D.; Suzumi, K. *Am. Chem. Soc.* **2008**, *130*, 1550–1551. b) Kamkaew, A.; Lim, S. I. Bee, H. B.; Kiew, L. Y.; Chung, L. Y.; Burgess, K. *Chem. Soc. Rev.* **2013**, *42*, 77–88. c) Awuah, S. G.; You, Y. *RSC Adv.* **2012**, *1*, 11169–11183. d) Ulrich, G.; Ziessel, R.; Harriman, A. *Angew. Chem. Int. Ed.* **2008**, *47*, 1184–1201. e) Imahori, H.; Norieda, H.; Yamada, I. Nishimura, Y.; Yamazaki, I.; Sakata, Y.; Fukuzumi, S. *J. Am. Chem. Soc.* **2001**, *123*, 100–110. f) Engelhardt, V.; Khuri, S.; Fleischhauer, Garcia-Iglesias, M.; Gonzalez-Rodríguez, D.; Bottari, G.; Torres, G.; Guldi, D. M.; Faust, R. *Chem. Sci.* **2013**, *4*, 3888–3892. g) C. Obondi, G. N. Lim, P. A. Karr, V. N. Nesterov, F. D'Souza, *Chem. Phys. Phys. Chem.* **2016**, *18*, 18187–18200.
- [14] a) V. Bandi, S. K. Das, S. G. Awuah, Y. You, F. D'Souza, *J. Am. Chem. Soc.* **2014**, *136*, 7571–7574; b) B. Dhokale, P. Gautam, S. M. Mobin, Misra, *Dalton Trans.*, **2013**, *42*, 1512–1518.
- [15] a) S. Paek, N. Cho, S. Cho, J. K. Lee, J. Ko, *Org. Lett.*, **2012**, *14*, 63; b) W. Z. Yuan, Y. Gong, S. Chen, X. Y. Shen, J. W. Y. Lam, P. Lu, Lu, Z. Wang, R. Hu, N. Xie, H. S. Kwok, Y. Zhang, J. Z. Sun, B. Tang, *Chem. Mater.*, **2012**, *24*, 1518. c) C. A. Wijesinghe, M. E. I. Khoully, M. E. Zandler, S. Fukuzumi, F. D'Souza, *Chem. Eur. J.* **2019**, *25*, 9629–9638.
- [16] a) M. Kivala, F. Diederich, *Acc. Chem. Res.*, **2009**, *42*, 235–248; b) Kato, F. Diederich, *Chem. Commun.*, **2010**, *46*, 1994–2006; c) Kivala, T. Stanoeva, T. Michinobu, B. Frank, G. Gescheidt, Diederich, *Chem. – Eur. J.*, **2008**, *14*, 7638–7647; d) A. Leliège, Blanchard, T. Rousseau, J. Roncali, *Org. Lett.*, **2011**, *13*, 3098–3101; T. Michinobu, N. Satoh, J. Cai, Y. Lia, L. Hanb, *J. Mater. Chem.* **2014**, *2*, 3367–3372; f) B. Esembeson, M. L. Scimeca, T. Michinobu, Diederich, I. Biaggio, *Adv. Mater.*, **2008**, *20*, 4584–4587.
- [17] B. Basumatary, A. R. Sekhar, R. V. R. Reddy, J. Sankar, *Inorg. Chem.* **2015**, *54*, 4257–4267
- [18] R. Misra, P. Gautam, S. M. Mobin, *J. Org. Chem.* **2013**, *78*, 12440–12452.
- [19] R. Misra, P. Gautam, *Org. Biomol. Chem.*, **2014**, *12*, 5448.
- [20] a) P. Gautam, B. Dhokale, S. M. Mobin, R. Misra, *RSC Adv.*, **2012**, *12105*–12107; b) Y. Chen, J. Zhao, H. Guo, L. Xie, *J. Org. Chem.* **2012**, *77*, 2192.
- [21] H. B. Gobeze, S. Kumer, F. D'Souza, M. Ravikanth, *Chem. Eur. J.* **2017**, *23*, 1546–1556.
- [22] J. R. Lakowicz, *Principles of Fluorescence Spectroscopy*, 3rd ed Springer, Singapore, 2006.
- [23] a) F. D'Souza, *J. Am. Chem. Soc.* **1996**, *118*, 9232–924. b) Q. Xie, Perez-Cordero, L. Echegoyen, L. J. Am. Chem. Soc. **1992**, *114*, 3978.
- [24] *Gaussian 09*, M. J. Frisch, G. W. Trucks, H. B. Schlegel, G. E. Scuseria, M. A. Robb, J. R. Cheeseman, V. G. Zakrzewski, J. A. Montgomery, R. E. Stratmann, J. C. Burant, S. Dapprich, J. M. Millam, A. D. Daniels, K. N. Kudin, M. C. Strain, O. Farkas, J. Tomasi, V. Barone, M. Cossi, R. Cammi, B. Mennucci, C. Pomelli, C. Adamo, S. Clifford, J. Ochterski, G. A. Petersson, P. Y. Ayala, Q. Cui, K. Morokuma, D. K. Malick, A. D. Rabuck, K. Raghavachari, J. B. Foresman, J. Cioslowski, J. V. Ortiz, B. B. Stefanov, G. Liu, A. Liashenko, P. Piskorz, I. Komaromi, R. Gomperts, R. L. Martin, D. J. Fox, T. Keith, M. A. Al-Laham, C. Y. Peng, A. Nanayakkara, C. Gonzalez, M. Challacombe, P. M. W. Gill, B. G. Johnson, W. Chen, M. W. Wong, J. L. Andres, M. Head-Gordon, E. S. Replogle, J. A. Pople, Gaussian, Inc., Pittsburgh PA, 2009.
- [25] D. Rehm, A. Weller, *Isr. J. Chem.*, **1970**, *8*, 259.

- [26] C. B. KC, G. N. Lim, V. N. Nesterov, P. A. Karr, F. D'Souza, *Chem. Eur. J.* **2014**, *20*, 17100-17112.
-

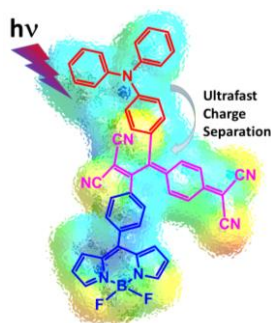
Received: ((will be filled in by the editorial staff))
Revised: ((will be filled in by the editorial staff))
Published online: ((will be filled in by the editorial staff))

Accepted Manuscript

Donor-Acceptor Interactions

Ultrafast charge separation in triphenylamine-BODIPY derived triads carrying centrally positioned, highly electron deficient, dicyanoquinodimethane or tetracyanobutadiene electron acceptors

P. Gautam, R. Misra*, M. B. Thomas, F. D'Souza*



In search of stronger electron acceptors: Newly synthesized molecular triads carrying centrally positioned dicyanoquinodimethane or tetracyanobutadiene electron acceptors are shown to promote ultrafast charge separation and recombination.